

Open-circuit and Short-circuit Fault Diagnosis and Fault Tolerant Strategy for Non-isolated Three-level Boost DC-DC Converters for Photovoltaic Energies Applications

Ait Ayad Imane*[‡], Elwarraki Elmotafa*, Baghdadi Mohamed*

Laboratory of Electrical Systems, Energy Efficiency and Telecommunications, Faculty of Sciences and Technologies, Cadi Ayyad University

(imane.aitayad@ced.uca.ma, m.elwarraki@uca.ac.ma, mohamed.baghdadi@ced.uca.ma)

‡

Corresponding Author; Ait Ayad Imane, Avenue Abdelkrim Khattabi, B.P. 511 - 40000, Tel: +212 678 45 79
83,imane.aitayad@ced.uca.ma

Received: 11.04.2023 Accepted: 24.06.2023

Abstract- Three Level Boost (TLB) DC-DC converters have been widely used in renewable energies, because of their advantages related to efficiency, volume, modularity, and inductor current ripples. To improve their reliability, a simple diagnosis method for switches Short-circuit (SC) and Open-circuit (OC) faults in a TLB converter and a fault-tolerant reconfiguration using only the output capacitor voltages sign features are presented. The capacitor voltages are thoroughly studied for both switches healthy and faulty modes. The presented method is robust, and no additional sensors are required. With the new approach, it's possible to locate the faulty switch, as well as determine if it's an OC or SC failure. As a result, the TLB converter is reconfigured to a conventional boost converter, ensuring service continuity by adding only a redundant switch as a remedy. The experimental results using the dSPACE DS1104 controller board validate the proposed diagnosis method.

Keywords Three level boost converter; Fault occurrence; Fault diagnosis; Detection and location; Fault tolerant.

1. Introduction

In recent decades, Multi-level boost DC-DC converters have been received attention with increasing applications such as renewable energies, electric vehicles and fuel cell [1-10]. So the converters must be reliable because a problem in these circuits might cause failure or malfunction throughout the chain. The power switches are the most susceptible to faults due to their sensitive operation. Therefore, this paper focuses on detecting and locating the power switch failures to develop a fault tolerant topology to optimize faulty modes and ensure service continuity. An open or a short-circuit in a power switch is the most prevalent type of malfunction. Overvoltage or temperature overshoot might induce avalanche stress or an incorrect gate-driver to trigger the OC and SC faults [11].

Power switch faults diagnosis in DC/DC converters has become an emerging research topic in electrical engineering that has experienced strong development.

Several authors have been interested in DC/DC converters diagnosis; In [12], the authors have proposed a diagnosis technique for OC and SC fault of the power switch and diode in non-isolated DC-DC converters. The proposed method's theoretical and experimental applications for Buck, Boost and Buck-Boost converters have been introduced. In [13-16], an OC and SC fault diagnosis system with fault tolerance ability for DC-DC Boost converter power switch in a PV system has been presented. In [17], a detection algorithm for non-isolated DC-DC converters and a fault-tolerant topology based on a redundant switch have been proposed. Both types of switch failure could be detected.

Experimental tests have been done and confirmed the proposed approach.

A diagnosis technique using the input current for interleaved boost converter (IBC) has been addressed in [18-22]. There has been researched on the use of the output voltage harmonic amplitude to diagnose an open-circuit in a three-phase interleaved buck DC-DC converter [23]. OC fault detection and fault-tolerant strategy were presented in [24] for a TLB converter in a PV system. The authors have proposed a reconfiguration solution, which consists of the arrangement of two energy sources by adding a Triac. In [25], the detection only of the CO type fault has been proposed for a TLB converter applied in a wind power generation system.

In this paper, it is focused on TLB switches faults diagnosis. The main contribution of the presented work is focusing on both switches OC and SC faults diagnosis and proposing a fault tolerant strategy for the TLB converter to ensure the service continuity of the PV system. Fig. 1 shows the proposed TLB fault tolerant converter.

The fault detection is ensured by the capacitors voltages V_{c1} and V_{c2} used for output capacitors' balance control. Suppose the capacitor imbalance voltage is lower or higher than a well-defined threshold to differentiate faulty mode type. In that case, the faulty switch is detected, and fault type is identified. As a result, no more voltage sensors will be required, as seen in the proposed technique design in Fig. 6. The introduced fault-tolerant converter performs as a TLB converter under normal conditions. PWM signals phase-shifted by 180° are used to control the switches T_1 and T_2 while the T_3 switch is not controlled. A two-level boost converter is configured when the converter is in defective mode. When applying PWM control, T_3 is the only one that is controlled. On an experimental setup, the proposed fault-tolerant method was tested for all possible scenarios. The experimental results show that the proposed fault detection approach effective for all failure modes. Here are the sections that make up the rest of the paper: TLB converter topology is discussed in Section 2. Section 3 introduces the principle of failure diagnosis and fault-tolerant reconfiguration. Section 4 concludes with presenting the experimental results and the subsequent discussions. Finally, a conclusion is presented in section 5

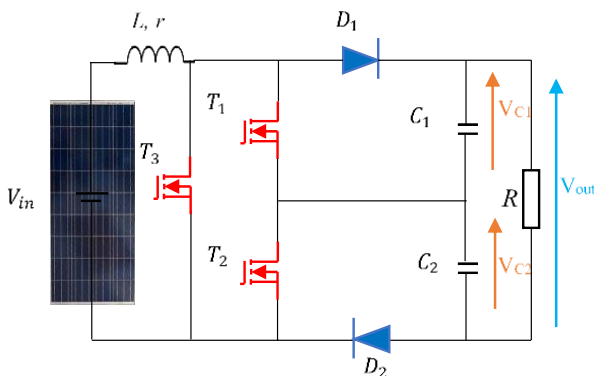


Figure 1. Proposed TLB converter fault tolerant.

2. TLB Converter Topology Operation

Three level boost converter is a conventional boost interleaving topology in order to decrease the input current ripple and the voltage stress on the power switches [26].

The TLB converter circuit diagram comprises two power switches, T_1 and T_2 (MOSFET), two rapid diodes D_1 and D_2 , an input inductor L and two output capacitors C_1 and C_2 . R is the resistive load. V_{in} is the voltage supply and V_{out} is the output converter voltage. The power switches are controlled by a duty cycle d , but their PWM (Pulse width modulation) signals are a phase difference of 180° . Therefore, four switching modes are possible, as shown in Fig. 2. For simplicity, the PV generator is replaced by a DC source

2.1. Normal Operating Principle

In mode 1: switches T_1 and T_2 are closed. The diodes D_1 and D_2 are opened. Thus, there is no energy transfer between the source and the load. The inductor is connected with the voltage supply and stores up energy. The capacitors are discharging, as presented in Fig. 2(a).

In mode 2: T_1 is closed, and T_2 is opened. The inductor current flows through the diode D_2 . C_1 is discharging, and C_2 is charging, as presented in Fig. 2(c).

In mode 3: T_2 is closed, and T_1 is opened. In this mode, the current flows through the diode D_1 , as illustrated in Fig. 2(b).

In mode 4: T_1 and T_2 are closed, as shown in Figure 2(d). The inductor current flows through the both diodes. Therefore, the inductor energy is transferred to the converter load. The output capacitors are in charging mode.

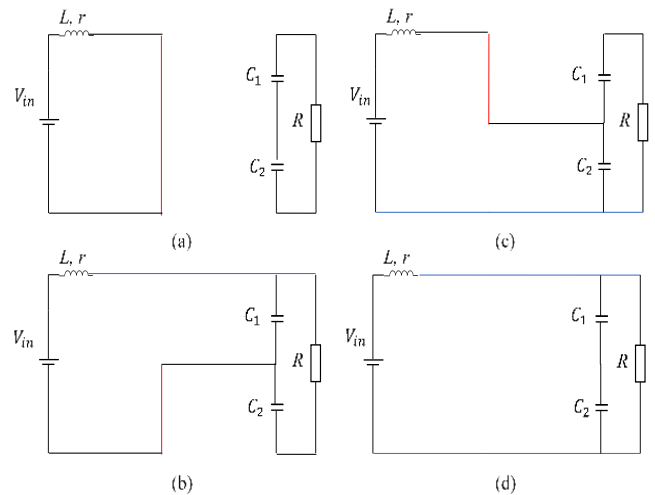


Figure 2. Normal operating modes in TLB converter: (a) Mode 1; (b) Mode 2; (c) Mode 3; and (d) Mode 4.

2.2. Faulty Mode Analysis

This section presents the TLB converter behaviour under fault conditions of power switches open/short-circuit faults. As illustrated in Table 1, four scenarios could be identified

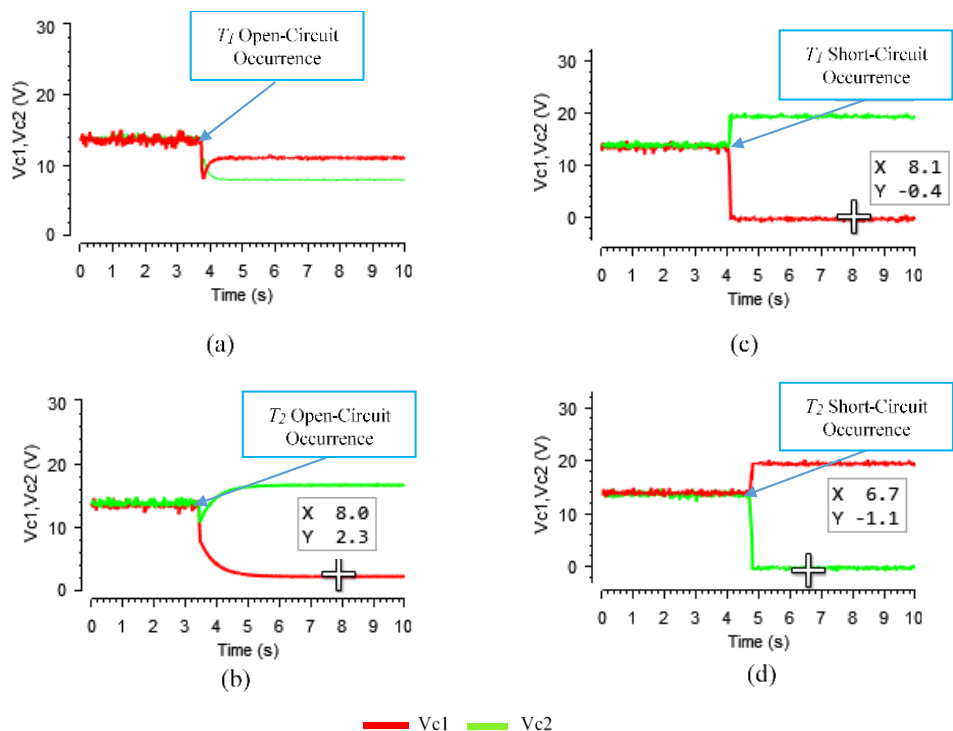


Figure 3. Experimental capacitor voltages before and after fault occurrence: (a) Switch T_1 and (b) Switch T_2 for OC fault case; (c) Switch T_1 and (d) Switch T_2 for SC fault case

during faulty mode: OC fault of T_1 , SC of T_1 , OC of T_2 , and SC of T_2 . Figure 3 depicts the capacitor voltages before and after fault occurrence.

The capacitor voltages tests are made experimentally in our laboratory for a realized TLB converter. Table 2 shows the converter parameters.

For experimental tests, the switch OC and SC faults were realized by disabling the gate drivers and turning on continuously either of the two switches. Then, the capacitor voltages behaviour is observed and analyzed. When an OC or SC fault occurs, the capacitor voltages are not more equilibrated, as illustrated in Fig. 3 with different values conditions.

As it can be noticed, when a fault appears, there is a large capacitor imbalance voltage. Therefore, a diagnosis signature of switches OC and SC faults can be defined using this imbalance.

To validate the diagnosis signature chosen under transient conditions, the capacitors voltages balance is measured experimentally in the presence of dynamic conditions, such as a varying load and a varying supply voltage.

Fig. 4 and Fig. 5 present the waveforms of capacitors voltages under a sudden input voltage variation and a sudden load variation respectively. According to Fig. 4(b) and Fig.

5(b), the capacitors voltages remain balanced in the presence of dynamic conditions.

Therefore, the proposed fault diagnosis signature is validated and can give a health diagnosis.

Table 1. Possible switch failures in TLB converter.

Faulty mode	Switch T1	Switch T2
1	OC	-
2	SC	-
3	-	OC
4	-	SC

Table 2. TLB converter parameters.

Parameter values	Value
V_{in}	16V
C_2, C_1	470 μ F
R	120 Ω
L	10 mH
r	0.25 m Ω
F	10 kHz

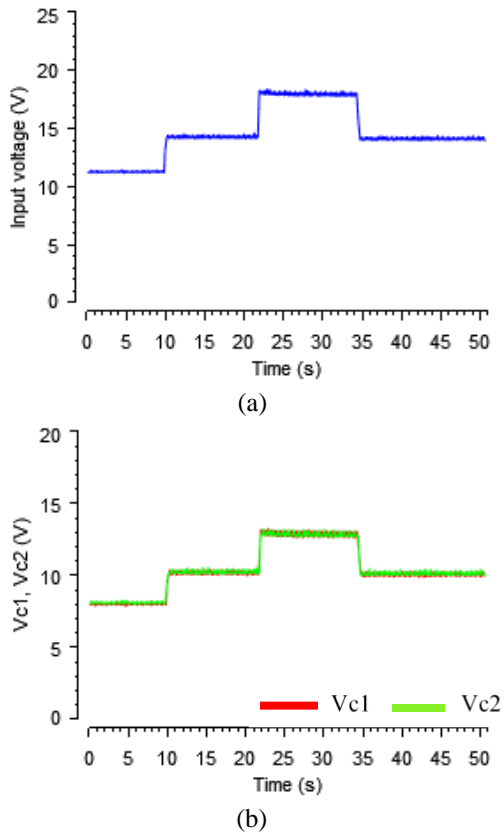


Figure 4. Experimental capacitor voltages under varying input voltage: (a) Input voltage (b) Capacitor voltages

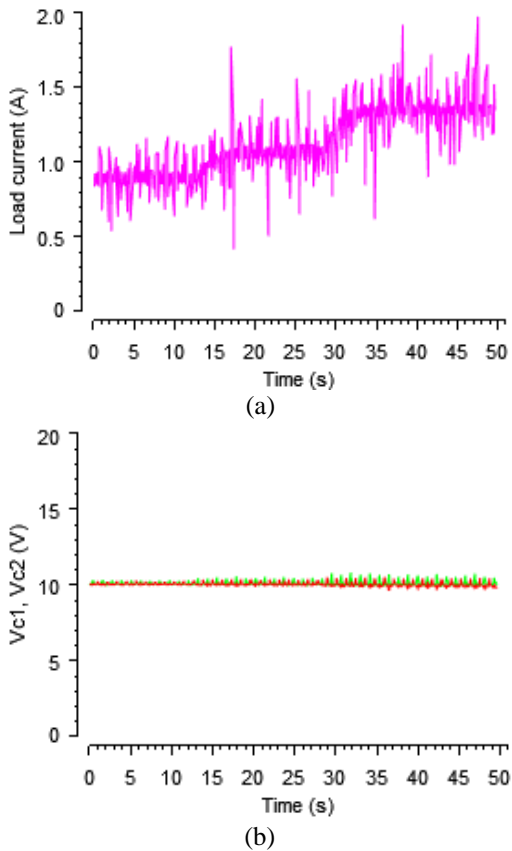


Figure 5. Experimental capacitor voltages under varying load: (a) Load current (b) Capacitor voltages

3. Proposed Fault Diagnosis Technique and Tolerant Reconfiguration Design

Three level boost converter is a conventional boost interleaving topology in order to decrease the input current ripple and the voltage stress on the power switches [26].

The proposed diagnosis method design is detailed in Fig. 6. To detect and locate (the topology studied has two power switches) the fault occurrence, capacitor voltages are measured, and the difference E between V_{c1} and V_{c2} is used as fault diagnosis controller inputs.

$$\text{Where, } E = V_{c1} - V_{c2} \tag{1}$$

During normal operation, F is equal to zero and \bar{F} is equal to 1, where fault signal F indicates occurrence fault. The power switches $T1$ and $T2$ are controlled, while the power switch $T3$ is uncontrolled because the latter is multiplied by F .

The PWM control signal for switch $T1$ is generated using a duty cycle d during normal operation. Then, the PI capacitor voltage balance output is added to the duty cycle d to provide a PWM signal for switch $T2$.

When a fault occurs, the fault diagnosis algorithm output F is equal to 1 and \bar{F} is equal to 0. Then, the PWM control signals of $T1$ and $T2$ are disabled because they are multiplied by \bar{F} , and the $T3$ control signal is enabled. The $T3$ is controlled using the same duty cycle d in order to keep the same power.

Variables $T1\text{-OCF}$, $T1\text{-SCF}$, $T2\text{-OCF}$, and $T2\text{-SCF}$ indicate respectively OC fault of $T1$, SC of $T1$, OC of $T2$, and SC of $T2$. These variables are equal to zero during normal operation.

Figure 7 presents the fault diagnosis flowchart. The difference E between V_{c1} and V_{c2} is calculated, and then it is compared to a predefined threshold K in order to detect the fault when it occurs. After that, the capacitor voltage is compared to a second predefined threshold C in order to determine the fault type.

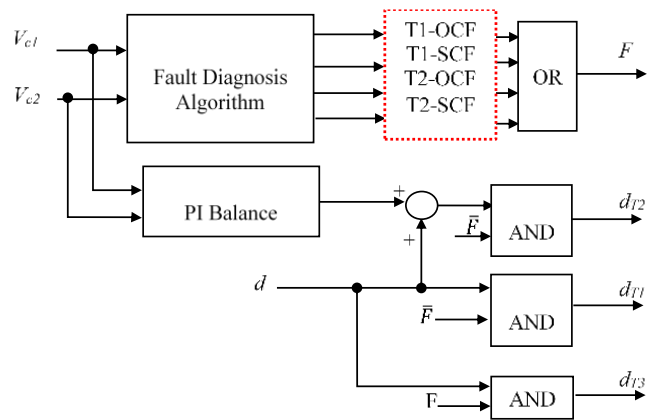


Figure 6. Proposed fault tolerant method design.

During experimental tests, the K and C thresholds were empirically chosen. For K, the 7% value of capacitor voltages was good for optimizing the diagnosing time.

For C, as shown in Fig. 3, the capacitor voltage is always less than zero in the short circuit case, and it is greater than zero in the open circuit case. Thus, C is chosen relative to zero.

After fault detection and faulty switch identification, the converter operates as a two-level boost converter. Then, the service continuity is ensured, and the energy losses are optimized.

4. Experimental Results and Discussions

This section presents experimental tests to validate the fault detection technique and fault tolerant reconfiguration for the TLB converter realized in our laboratory. The proposed method is implemented in real-time via the dSPACE DS1104 controller board using its monitor software (ControlDesk) and Matlab/Simulink software.

Control Desk is an interface that allows you to visualize in real time the various variables of the control strategy developed in Simulink, and to modify the operating mode parameters of Simulink blocks.

The dSPACE DS1104 board from R&D operates as an interface between the computer and the CBTN with driver stage, using Matlab/Simulink software. Its real-time, PowerPC-based system and input/output interfaces make it a perfect solution for rapid control prototyping. The dSPACE 1104 controller board is interfaced with the systems using the Real Time Interface (RTI), which is a link between the dSPACE hardware and the MATLAB/Simulink software. The latter is used to develop the control system using Simulink blocks, and to simulate it. Thus, the developed controller described in the previous section is easily implemented in Simulink using the Real-Time Workshop (RTW) functionality integrated into the Simulink environment.

It should be noted that it is recommended that the step time ($10 \mu s$ chosen in this work) used by the dSPACE board be sufficiently small compared to the switching period ($100 \mu s$ in this work) of the converter. This makes it possible to accurately capture the dynamic behavior of the control system. The dSPACE DS1104 architecture is given in Fig. 8.

Fig. 9 presents a block diagram of the experimental setup; dSPACE Analog/Digital converters (ADC_C5 and ADC_C6) receive the measured capacitors voltages VC1 and VC2 by the voltage sensors. After introducing a fault at different times by continually enabling or disabling the gate signal of the switch chosen. Based on the difference between VC1 and VC2, the proposed fault tolerant controller modeled in Simulink Real Time detects and identifies the faulty switch and provides the suitable duty cycles dT1, dT2, and dT3. These variables are used as inputs of the dSPACE 1104_slave_PWM generator to directly produce the PWM

control signals to control the redundant switch T3 as a remedy, while both switches are not controlled.

The experimental bench is illustrated in Fig. 10 in detail. It is composed of a TLB converter whose IRFP460A are used as power switches, of a gates driver IR2110 and voltage sensors. The IRFP460A switch and IR2110 are characterized by a high speed power switching, which ensures that the system operates with an optimized switching speed.

Table 3 lists all the components used in the CBTN, indicating their references.

To visualize in real-time the different variables of the fault diagnosis strategy developed in Simulink and modify the parameters of the operating mode of the Simulink blocks, the interface dSPACE ControlDesk is used.

Table 3. List of TLB converter component

Component	Reference	Value
MOSFET	IRFP460A	$V_{DS} = 500 \text{ V}$, $I_D = 20 \text{ A}$, $R_{ds} = 0.27 \Omega$
Diode Schottkey	STPS20120D	$I_F = 20 \text{ A}$, $V_{RRM} = 120 \text{ V}$ $V_F = 0.54 \text{ V}$
Inductor	37-C5311301 ROHS	10 mH, $r = 23 \text{ m}\Omega$
Capacitors C ₁ and C ₂	KCAPXYN GS85°C	700 μF , 63 V

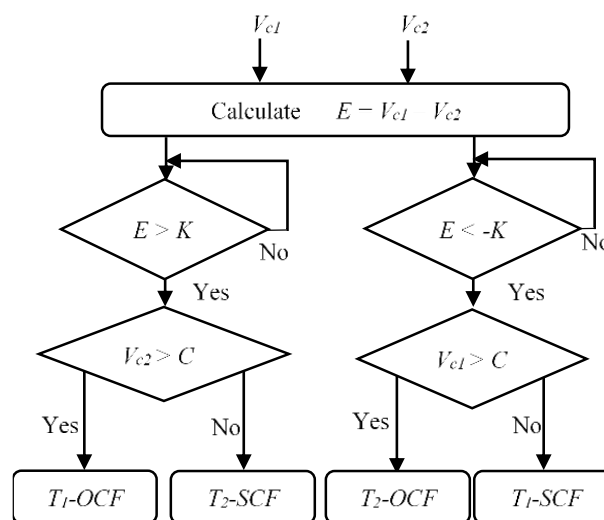


Figure 7. Fault diagnosis flowchart

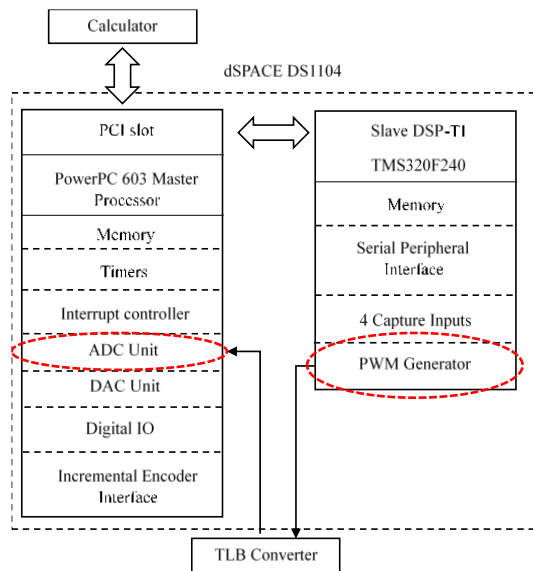


Figure 8. Blocks of the dSPACE board

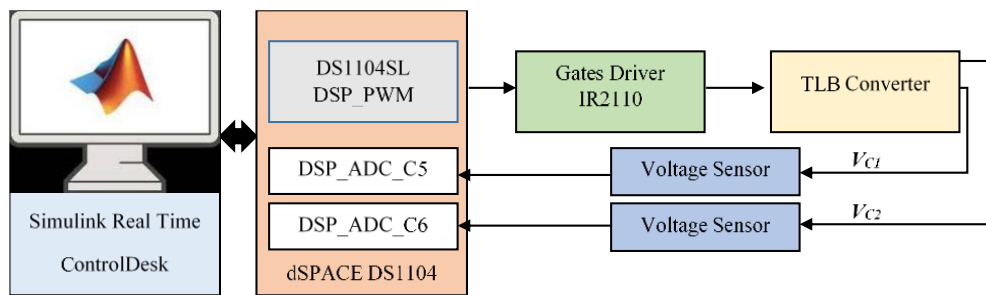


Figure 9. Schema blocks of experimental setup.

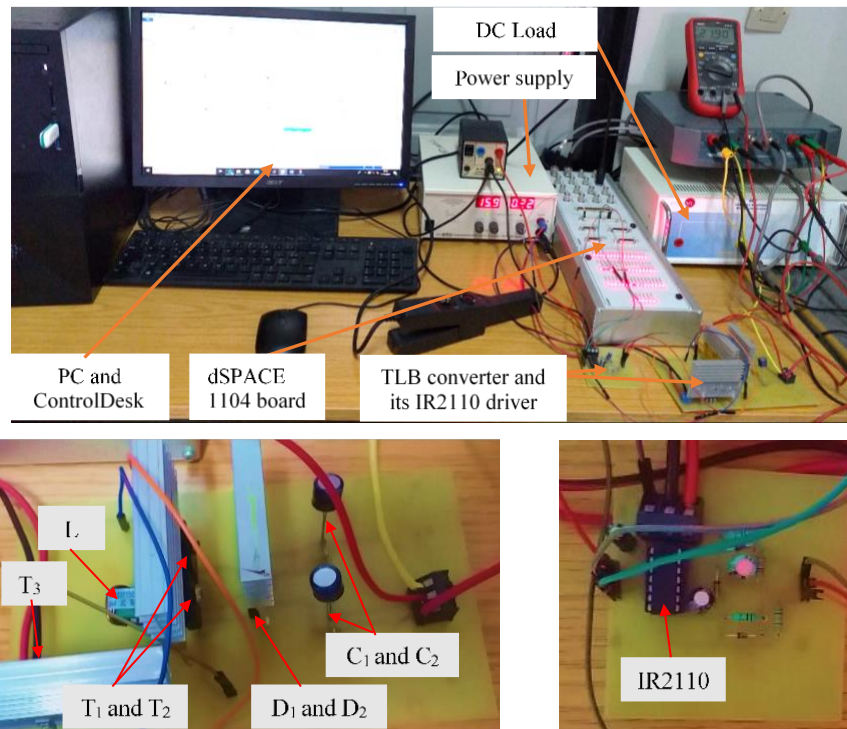


Figure 10. Setup experimental

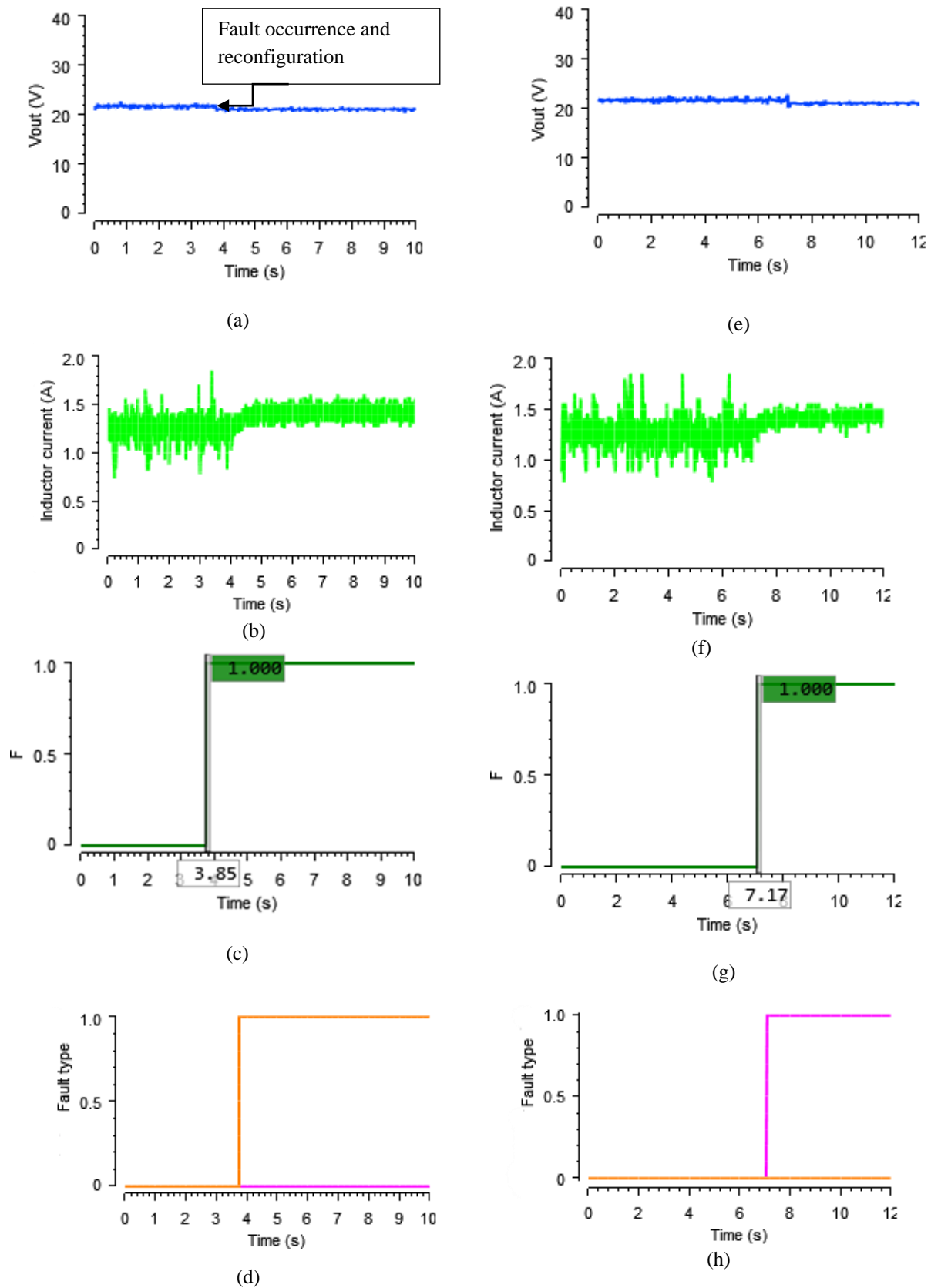


Figure 11. Experimental results of power switch T1 failures: (a) Output voltage; (b) Inductor current; (c) fault detection signal; and (d) Fault type signal for OC fault case; (e) Output voltage; (f) Inductor current; (g) fault detection signal; and (h) Fault type signal for SC fault case

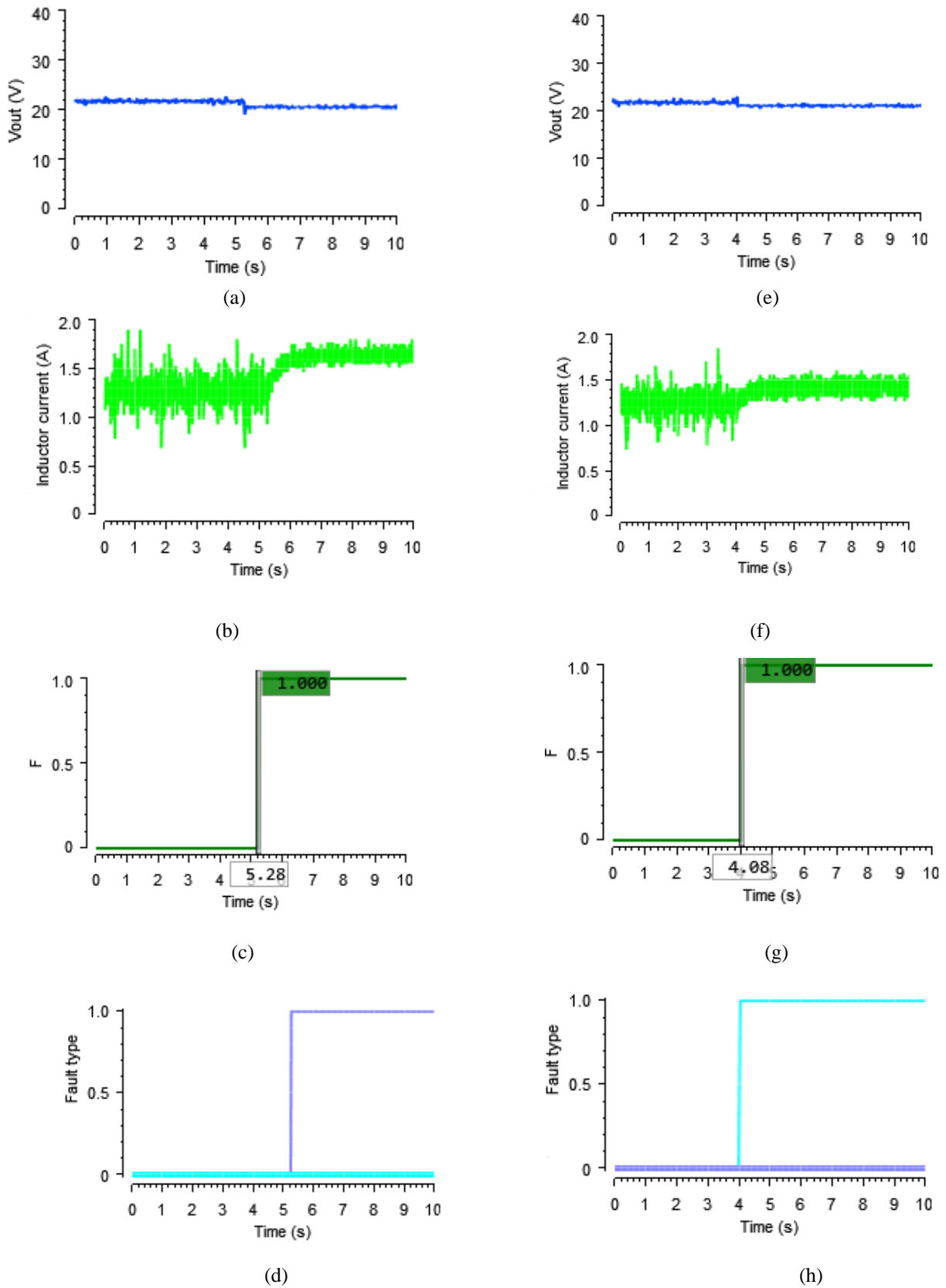


Figure 12. Experimental results of power switch T2 failures: (a) Output voltage; (b) Inductor current; (c) fault detection signal; and (d) Fault type signal for OC fault case; (e) Output voltage; (f) Inductor current; (g) fault detection signal; and (h) Fault type signal for SC fault case

Table 4. Comparison of fault diagnosis methods

Reference	Converter	Detection parameter	Fault Type	Experimental validation	Reconfiguration capability	Cost
[27]	Boost converters	Output voltage	OC	No	No	Low
[28]	Output-series Interleaved boost	Inductor current and output voltage	OC	Yes	Yes	Low
[29]	Flying capacitor Buck-boost converters	Capacitor voltage and current	SC and OC	Yes	Yes	Low
[24]	TLB converter	Capacitors voltages	OC	Yes	Yes	High
[25]	TLB converter	Capacitors voltages	OC	No	Yes	High
[30]	TLB converter	Capacitors voltage	OC	NO	Yes	High
Proposed method	TLB converter	Capacitor voltage	SC and OC	Yes	Yes	Low

Experimental results of different possible cases study are represented in Figs. 11 and 12. In the first case study presented in Fig. 11, after that T1 OC fault occurs, the fault is detected very quickly. The faulty switch and switch fault types are identified as illustrated in Fig. 11(c) and Fig. 11(d), respectively. Then, the TLB converter was reconfigured to a conventional boost converter. Thus, the output voltage and the inductor current practically remain unchanged with a very low error, as shown in Fig. 11(a) and Fig. 11(b). Like the switch T1 OC fault case, the T1 CC fault and T2 CO/CC faults are detected rapidly, and output voltage and inductor current practically remain unchanged, as shown in Figs. 11(e), (f), (g), and (h) and Fig. 12 respectively

Table 4 compares some fault diagnostic approaches presented for DC-DC converter in the literature from different aspects including detection parameter, fault type, reconfiguration capability, and cost. Table 4 clearly shows that the proposed technique is beneficial in terms of fault identification capability, SC and OC detection, reconfiguration capability, and implementation cost. It should be noted that costs associated with the necessary additional sensors and diagnostic circuitry for fault detection are taken into consideration when comparing techniques from a cost perspective. Using this criterion, the methods can be classified into three categories: high cost, medium cost, and low cost.

By analyzing the experimental results, it can be seen that the proposed diagnosis method capability is confirmed. After the fault occurrence, the detection is considered fast, and the converter is reconfigured to a conventional boost converter with the same output voltage.

Therefore, this technique is used due to its simplicity, and its optimization of execution time, and it is also feasible for a higher voltage level topology because it does not depend on the converter's power.

5. Conclusion

This paper proposed a simple strategy for switch faults detection in a non-isolated TLB converter. The presented method's capability for detecting and identifying both TLB switches fault types is the main novelty of this technique. It is confirmed that the capacitor voltages contain some valid signatures for both open-circuit and short-circuit faults diagnosis of both switches. A software program is introduced in which the capacitor voltages are processed to provide four-fault type indicator signals. For each type of fault, including switch T1 OC and SC faults, and switch T2 OC and SC faults. The proposed technique is simple and cost-effective since it does not require any additional sensor; it requires only a redundant power switch. The detection delay of the proposed method for different faults is very low. Using some experiments carried out on realized TLB converter, the effectiveness of the proposed method was confirmed in terms of cost, fault detection and reconfiguration capability.

References

1. M. Afkar, R. Gavagsaz-Ghoachani, M. Phattanasak, J.-P. Martin, S. Pierfederici, "Proposed system based on a three-level boost converter to mitigate voltage imbalance in photovoltaic power generation systems", *IEEE Trans. Power Electron.* Vol. 37, pp. 2264-2282, 2022.
2. R. Tsuruta, T. Kataoka and T. Takuno, "Experimental Verification of a Front-End AC/DC Converter Capable of Stabilizing Ground Potential in a Multi-Level DC Distribution System," 2022 11th International Conference on Renewable Energy Research and Application (ICRERA), Istanbul, Turkey, 2022, pp. 219-223, doi: 10.1109/ICRERA55966.2022.9922674.
3. A. N. Fey, V. Leite and E. F. Ribeiro Romaneli, "A Low Power Photovoltaic Water Pumping System based on a DC-DC Step-up Converter and Standard Frequency Converters," 2020 9th International Conference on Renewable Energy Research and Application (ICRERA), Glasgow, UK, 2020, pp. 138-143, doi: 10.1109/ICRERA49962.2020.9242833.
4. A. Sahbani, K. Cherif, and K. B. Saad, "Multiphase Interleaved Bidirectional DC-DC Converter for Electric Vehicles and Smart Grid Applications", *International Journal of Smart Grid-ijSmartGrid*, 4(2), 2020, pp. 80-87..
5. H. Benbouhenni, Z. Boudjema, and A. Belaidi, "A direct power control of the doubly fed induction generator based on the three-level NSVPWM technique", *International Journal of Smart Grid-ijSmartGrid*, 3(4), 2019, pp. 216-225..
6. Z. A. Ghafour, A. R. Ajel and N. M. Yasin, "A New High Gain Quadratic DC-DC Boost Converter for Photovoltaic Applications," 2022 10th International Conference on Smart Grid (icSmartGrid), Istanbul, Turkey, 2022, pp. 137-144, doi: 10.1109/icSmartGrid55722.2022.9848749..
7. I. A. Ayad, E. Elwarraki, S. U. Ali, S. M. Qaisar, A. Waqar, M. Baghdadi, and A. Alzahrani, "Optimized Nonlinear Integral Backstepping Controller for DC-DC Three-Level Boost Converters", *IEEE Access*, vol. 11, pp. 49794-49805, 2023, doi: 10.1109/ACCESS.2023.3274773.
8. M. Lee, J.-S. Lai, "Fixed-frequency hybrid conduction mode control for three-level boost PFC converter", *IEEE Trans. Power Electron.* Vol. 36, pp. 8334-8346, 2021.
9. I. Ait Ayad, E. Elwarraki, M. Baghdadi, "Intelligent Perturb and Observe Based MPPT Approach Using Multilevel DC-DC Converter to Improve PV Production System", *Journal of Electrical and Computer Engineering*, pp. 1-13, 2018
10. M. Lee, C. Yeh, O. Yu, J. Kim, J. Choe, J. Lai, "Modeling and control of three-level boost rectifier based medium-voltage solid-state transformer for DC fast charger application", *IEEE Trans. Transp. Electrification*. Vol. 5, pp. 890-902, 2019.
11. G. K. Kumar, D. Elangovan, "Review on fault-diagnosis and fault-tolerance for DC-DC converters", *IET Power Electronics*, vol. 13, pp. 1-13, 2020.
12. H. Givi, E. Farjah, T. Ghanbari, "Switch and diode fault diagnosis in nonisolated DC-DC converters using diode voltage signature", *IEEE Trans. Ind. Electron.* Vol. 65, pp. 1606-1615, 2017.
13. D. R. Espinoza Trejo, E. Bárcenas, J. E. Hernández Diez, G. Bossio, G. Espinosa Pérez, "Open-and short-circuit fault identification for a boost dc/dc converter in PV MPPT systems", *Energies*, vol. 11, pp. 616, 2018.
14. D. R. Espinoza Trejo, S. Taheri, J. A. Pecina Sánchez, "Switch fault diagnosis for boost DC-DC converters in photovoltaic MPPT systems by using high-gain observers", *IET Power Electronics*, vol. 12; pp. 2793-2801, 2019.
15. E. Pazouki, Y. Sozer, J. A. De Abreu-Garcia, "Fault diagnosis and fault-tolerant control operation of nonisolated DC-DC converters", *IEEE trans. Ind. Applications*, vol. 54, pp. 310-320, 2017.
16. A. M. Silveira, R. E. Araújo, "A new approach for the diagnosis of different types of faults in dc-dc power converters based on inversion method", *Electric Power Systems Research*, vol. 180, pp. 106103, 2020.
17. E. Jamshidpour, P. Poure, S. Saadate, "Photovoltaic systems reliability improvement by real-time FPGA-based switch failure diagnosis and fault-tolerant DC-DC converter", *IEEE Transactions on Industrial Electronics*, vol. 62, pp. 7247-7255, 2015.
18. D. Guilbert, M. Guarisco, A. Gaillard, A. N'Diaye, A. Djerdir, "FPGA based fault-tolerant control on an interleaved DC/DC boost converter for fuel cell electric vehicle applications", *International journal of hydrogen energy*, vol. 40, pp. 15815-15822, 2015.
19. M. W. Ahmad, N. B. Y. Gorla, H. Malik, S. K. Panda, "A fault diagnosis and postfault reconfiguration scheme for interleaved boost converter in PV-based system", *IEEE Transactions on Power Electronics*, vol. 36, pp. 3769-3780, 2020.
20. E. Ribeiro, A. J. M. Cardoso, C. Boccaletti, "Open-circuit fault diagnosis in interleaved DC-DC converters", *IEEE transactions on power electronics*, vol. 29, pp. 3091-3102, 2014.
21. L. Kou, C. Liu, G. W. Cai, Z. Zhang, "Fault diagnosis for power electronics converters based on deep feedforward network and wavelet compression", *Electric Power Systems Research*, vol. 185, pp. 106370, 2020.
22. F. Bento, A. J. Marques Cardoso, "Open-Circuit Fault Diagnosis and Fault Tolerant Operation of Interleaved DC-DC Boost Converters for Homes and Offices", *IEEE Transactions on Industry Applications*, vol. 55, pp. 4855-4864, 2019.
23. P. Li, X. Li, T. Zeng, "A Fast and Simple Fault Diagnosis Method for Interleaved DC-DC Converters Based

on Output Voltage Analysis”, *Electronics*, vol. 10, pp. 1451, 2021.

24. E. Ribeiro, A. J. M. Cardoso, C. Boccaletti, “Fault-tolerant strategy for a photovoltaic DC--DC converter”, *IEEE transactions on power electronics*, vol. 28, pp. 3008-3018, 2013.

25. A. Nouri, I. Salhi, N. Essounbouli, E. Elwarraki, ,A. Haraoubia, “DC-DC Converter fault diagnostic in wind energy production system: Simulation study”, *Energy Procedia*, vol. 83, pp. 408-417, 2015.

26. I. A. Ayad, , E. Elwarraki, A. Nouri, “A self-tuning fuzzy PI controller for three-level boost converter”, 6th International Renewable and Sustainable Energy Conference, Rabat, pp. 1-6, 5-8 December 2018.

27. H. Abouobaida, Y. Abouelmahjoub, L. Oliveira-Assis, “New open-circuit fault detection in a DC-DC converter”, *Int Trans Electr Energ Syst*, pp. 13094 (2021).

28. L. Xu, R. Ma, R. Xie, J. Xu, Y. Huangfu, F. Gao, “Open-Circuit Switch Fault Diagnosis and Fault-Tolerant Control for Output-Series Interleaved Boost DC-DC Converter”, *IEEE Trans. Transp. Electrification*, vol. 7n No. 4, pp. 2054-2066, 2021.

29. S. Tang, X. Yin, D. Wang, C. Zhang, Z. Shuai, X. Yang, Z. John Shen, J. Wang, “Detection and identification of power switch failures for fault-tolerant operation of flying capacitor Buck-boost converters”, *Microelectronics Reliability*, vol. 88, pp. 1236-1241, 2018.

30. A. Nouri, I. Salhi, S. El Beid, N. Essounbouli, and E. Elwarraki, “A fault tolerant strategy for multilevel dc-dc converters to improve the PV system efficiency”, *IFAC-PapersOnLine*, vol. 49, No. 12, pp. 704-709.